PHILOSOPHICAL TRANSACTIONS OF THE ROYAL SOCIETY A MATHEMATICAL, PHYSICAL & ENGINEERING SCIENCES

Mineral–microbe interactions in deep-sea hydrothermal systems: a challenge for Raman spectroscopy

J. A. Breier, S. N. White and C. R. German

Phil. Trans. R. Soc. A 2010 **368**, 3067-3086
doi: 10.1098/rsta.2010.0024

PHILOSOPHICAL TRANSACTIONS OF THE ROYAL SOCIETY A

Phil. Trans. R. Soc. A (2010) **368**, 3067–3086
doi:10.1098/rsta.2010.0024

Review

Mineral–microbe interactions in deep-sea hydrothermal systems: a challenge for Raman spectroscopy

By J. A. Breier*, S. N. White and C. R. German

Woods Hole Oceanographic Institution, Woods Hole, MA 02543, USA

In deep-sea hydrothermal environments, steep chemical and thermal gradients, rapid and turbulent mixing and biologic processes produce a multitude of diverse mineral phases and foster the growth of a variety of chemosynthetic micro-organisms. Many of these microbial species are associated with specific mineral phases, and the interaction of mineral and microbial processes are of only recently recognized importance in several areas of hydrothermal research. Many submarine hydrothermal mineral phases form during kinetically limited reactions and are either metastable or are only thermodynamically stable under *in situ* conditions. Laser Raman spectroscopy is well suited to mineral speciation measurements in the deep sea in many ways, and sea-going Raman systems have been built and used to make a variety of *in situ* measurements. However, the full potential of this technique for hydrothermal science has yet to be realized. In this focused review, we summarize both the need for *in situ* mineral speciation measurements in hydrothermal research and the development of sea-going Raman systems to date; we describe the rationale for further development of a small, low-cost sea-going Raman system optimized for mineral identification that incorporates a fluorescence-minimizing design; and we present three experimental applications that such a tool would enable.

Keywords: hydrothermal; mineralogy; optical instruments; Raman spectroscopy

1. Introduction

It is a case of historical fortune that Darwin lived in a time before deep-diving submersibles. This spared him the potential distraction of having to reconcile his thoughts on Galapagos finches with observations of the bizarre chemosynthetic ecosystems waiting be found on the seafloor just 450 km to the northwest of those birds. If Darwin had taken part in the cruise of Corliss *et al.* (1979), 142 years after his own voyage to the Galapagos, he might have dived in the submersible *Alvin* to the Rose Garden hydrothermal fields of the Galapagos Rift, and witnessed these exotic, toxic, but energy-rich environments

*Author for correspondence (jbreier@whoi.edu).

One contribution of 12 to a Theme Issue 'Raman spectroscopic approach to analytical astrobiology: the detection of key geological and biomolecular markers in the search for life'.

that are dominated by sulphide mineral formations and host fauna previously unknown to science, including metre-long vestimentiferan tubeworms and large vesicomyid clams and bathymodiolid mussels that can themselves extend to tens of centimetre in length (Fisher 1995; Hessler & Kaharl 1995). Life at these settings is uniquely adapted. For example, vestimentiferan adults have no digestive track and vesicomyids have only a limited ability to filter feed; instead, they have evolved to rely on endosymboitic chemosynthetic microbes for nourishment (Fisher 1995). In fact, the whole deep-sea vent ecosystem thrives on energy derived by *chemo*synthetic micro-organisms from oxidation of the reduced species that are emitted at hydrothermal vents. This flux of reduced chemicals is also significant in its own right, being one of the main avenues of chemical exchange between the lithosphere and the oceans and on a par with riverine fluxes and aeolian dust deposition for a number of elements (Kadko 1993; Elderfield & Schultz 1996; German & Von Damm 2003). A modern Darwin would surely have done well in such a situation, but the vent environment is so unique and difficult to study, that even after 32 years of modern scientific investigation, we do not fully understand it.

Areas of open research concern the exchange of material between the lithosphere and the oceans, the extent of the deep-sea chemosynthetic biosphere and the mechanisms by which records of hydrothermal discharge are created and preserved in massive sulphide and metalliferous sediment deposits. The interactions between mineral and microbial processes are important to all of these topics and occur with distinct variations in three key 'end-member' hydrothermal sub-environments: low-temperature (less than 20°C) diffuse flow, high-temperature (more than 280°C) vents and hydrothermal plumes (figure 1). These sub-environments provide very different examples of microbial activity, mineral reactions and their relationships. Low-temperature hydrothermal discharge promotes the growth of large microbial mats, often tens of centimetre thick. Biomass here is high while mineral mass is low—but mineral crusts often form at the mat–seawater interface and the availability of mineral substrates may influence mat development. High-temperature hydrothermal discharge promotes the growth of massive sulphide chimneys where mineral mass is high and biomass is low. Nevertheless, distinct microbial species inhabit the chemical and thermal niches within these chimneys and may also influence their structure. Finally, the dissolved and particulate products of venting are discharged to the water column through hydrothermal plumes where mineral particles can form rapidly and abiotically. Even here, however, a growing body of evidence suggests that microbes are active, playing roles that may previously have been overlooked.

Past studies have largely relied on *ex situ* bulk elemental and mineralogical measurements to elucidate the geochemical processes that occur in these systems. These however, shed only partial light on how such processes proceed: the hydrothermal supply of dissolved chemical constituents varies with time and between vents; speciation and oxidation rates vary with seawater redox conditions and vent-fluid composition; and the potential for non-equilibrium phases (e.g. mackinawite, greigite, wurtzite), and those readily oxidized by abiotic and biotic processes, to be important raises the possibility that all *ex situ* analyses may be biased towards thermodynamically stable and oxidized phases (e.g. Scott & Barnes 1972; Maginn *et al.* 2002; Fortin & Langley 2005). Complimentary

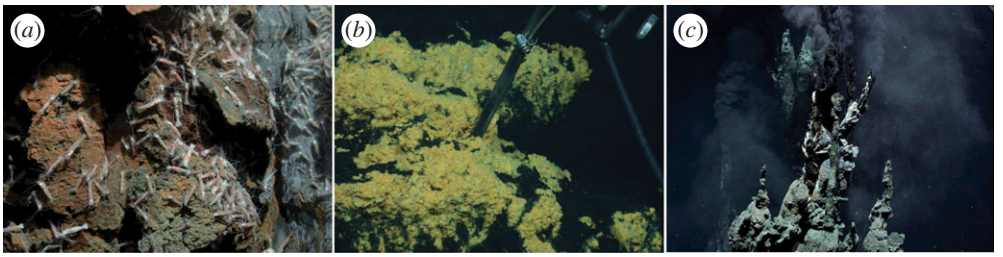

Figure 1. Mineral and microbial processes occur with distinct variations in several key hydrothermal sub-environments: (*a*) massive sulphide chimneys, (*b*) microbial mats and (*c*) hydrothermal plumes. Images courtesy of the National Science Foundation (NSF) Ridge 2000 program; Woods Hole Oceanographic Institution; C. R. Fisher, Pennsylvania State University; and A. L. Reysenbach, Portland State University. Images were acquired with support from NSF grants OCE02-40985, NSF OCE-0728391, OCE-0752469 and OCE-0751839.

techniques are required that can observe not only the composition of the phases present, but also the bonding within them—all *in situ*. For *in situ* speciation measurements, laser Raman spectroscopy has great potential. A particular strength of Raman spectroscopy is that it allows for non-invasive, non-destructive identification for many of the minerals present in hydrothermal systems. This would allow for reliable measurements of thermodynamically unstable phases to be made, *in situ*, and for long-term variations in mineral speciation to be monitored. Particular advantages would be the ability to (i) monitor mineralogical changes within hydrothermal chimney walls over time scales of months to years, (ii) identify mineral occurrence and speciation during vertical profiles through microbial mats, and (iii) track chemical transformations of Fe/Mn-rich material within evolving hydrothermal plumes, including the very earliest stages (less than or equal to 1 h) while the plume is still rising above a vent site, as well as during the following days and weeks as plume material is dispersed through the water column and settles to the seafloor. Such an approach would greatly improve our understanding of (i) the chemical evolution of hydrothermal systems themselves, (ii) the structure and biogeochemical cycling within microbial mats, and (iii) the impact of hydrothermal venting upon global ocean chemistry.

Sea-going Raman systems have been built (Battaglia *et al.* 2004; Brewer *et al.* 2004; Schmidt *et al.* 2004) and deployed to manually analyse gases (White *et al.* 2006*a*); synthetic and natural clathrate hydrates (Hester *et al.* 2006, 2007); and minerals, fluids and bacterial mats at hydrothermal vents (White *et al.* 2006*b*; White 2009). Laboratory testing has proven the ability to quantitatively, and autonomously distinguish many minerals typically found at deep-sea hydrothermal vents, even minerals with similar chemical compositions (figure 2; Breier *et al.* 2009*a*). Several instrument packages have been, or are being, developed that could interface with sea-going Raman systems in order to monitor and probe hydrothermal chimney structures, profile microbial mats (e.g. White *et al.* 2005) and analyse suspended or sinking hydrothermal plume particles (Bishop 2009; Breier *et al.* 2009*b*).

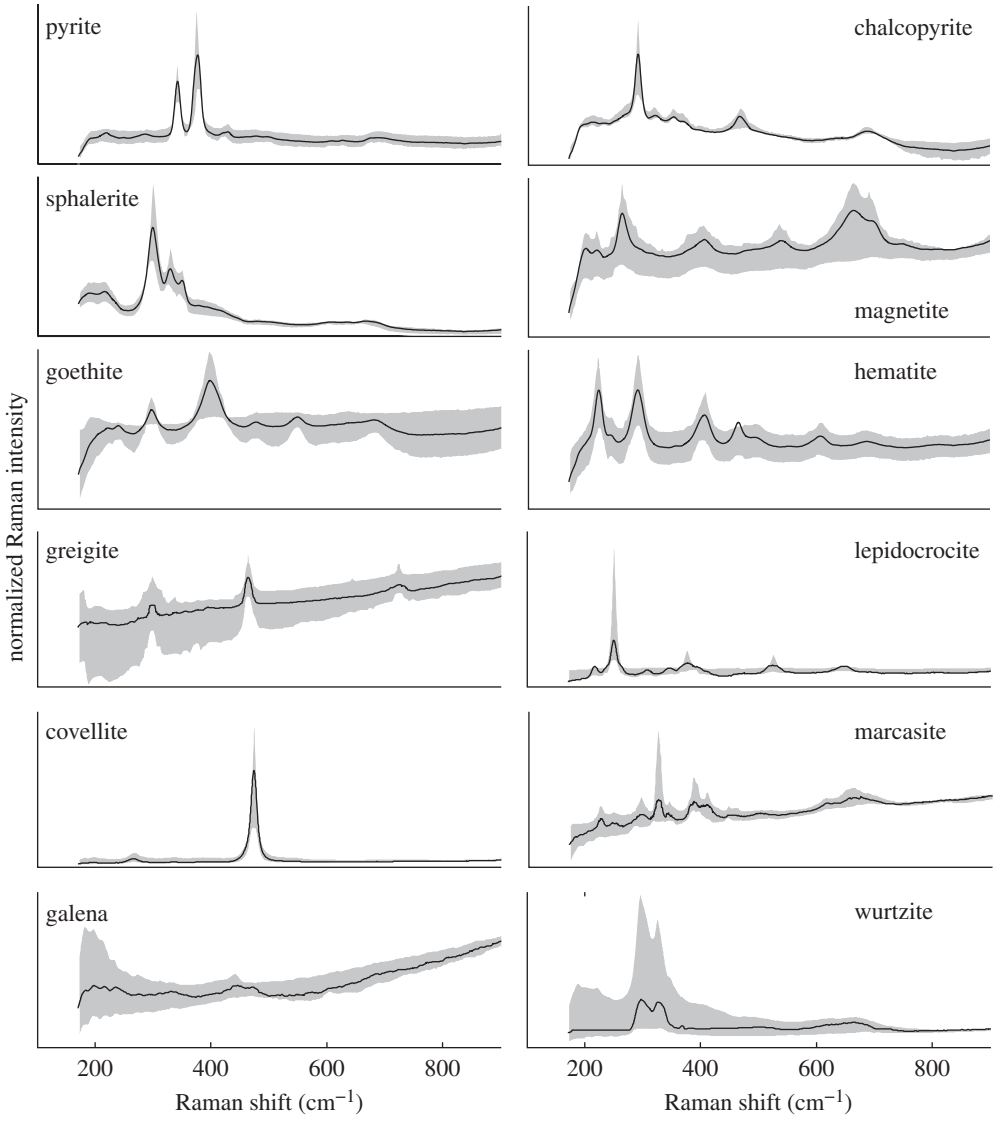

Figure 2. Raman spectra of minerals common in deep-sea hydrothermal systems, collected in the laboratory from prepared mineral standards and solid test specimens. Laboratory testing has shown spectrum shape, not absolute peak intensities, is sufficient to distinguish the majority of these minerals from each other (Breier *et al.* 2009*a*). Spectra have been normalized to one standard deviation of their individual intensity distributions, the black line is the median and the grey region denotes the 25th to 75th quantiles of the collected spectra.

Two technical issues still limit the use of laser Raman spectroscopy in the deep sea: system size and the issue of fluorescence. The most used sea-going Raman system built to date (Brewer *et al.* 2004) is a modified version of a commercially available laboratory Raman package, which requires a large fraction of a typical scientific submersible's payload. More compact commercial

packages are available, and other sea-going Raman systems being developed are smaller (Battaglia *et al.* 2004; Schmidt *et al.* 2004). Further optimization of size is desirable and would enable a greater range of deployment modes. More importantly, the presence of fluorescence-inducing organic matter and transition metals, which are ubiquitous in the vent environment, cannot be controlled or effectively eliminated *in situ*. Thus, there is a need for a purpose-built deep-sea laser Raman system that is both compact and incorporates fluorescence mitigating strategies. In this paper, we summarize the scientific needs, review the application of laser Raman spectroscopy in the deep sea and related technical developments, present the characteristics of a purpose-built laser Raman system for hydrothermal mineral analysis, including strategies for both minimizing system size and mitigating fluorescence, and describe the experiments that would be enabled by such a system.

2. Deep-sea hydrothermal systems

Hydrothermal circulation was recognized as an important pathway for chemical exchange between the lithosphere and the global ocean even prior to the discovery of mid-ocean ridge hydrothermal venting (Wolery & Sleep 1976; Corliss *et al.* 1979). At mid-ocean ridges and related geologic features (e.g. back-arc spreading centres), geothermal heat drives convection cells of seawater deep into fractured, permeable young ocean crust. Water–rock reactions significantly alter seawater chemistry during this process; it becomes reducing and acidic and is enriched in dissolved metals and volatile compounds. As hydrothermal fluid, it is discharged back to the oceans in the form of (i) focused high-temperature venting and (ii) diffuse patches of low-temperature discharge (Alt 1995; Tivey 1995).

At the seafloor, the mixing of high- (more than 300°C) and intermediate- (100–300°C) temperature hydrothermal discharge and seawater (2–4°C) results in rapid, profuse, mineral precipitation and the growth of massive sulphide deposits (Haymon & Kastner 1981; Janecky & Seyfried 1984; Hannington *et al.* 1995). A number of different sulphide structures and morphologies form depending on hydrothermal fluid composition, temperature, velocity, the degree of mixing with seawater and potentially biotic factors (Hannington *et al.* 1995; Tivey 1995). The conceptual model of high-temperature 'black smoker' chimney formation involves two stages (Goldfarb *et al.* 1983; Haymon *et al.* 1993; Tivey 1995). Stage I occurs when no previous structure exists, and involves the formation of a porous anhydrite conduit lattice during unrestricted mixing of seawater and vent fluid exiting the seafloor as a buoyant jet. Stage II occurs subsequently, as mixing of seawater and vent fluid is reduced by the presence of the porous anhydrite wall, and involves the precipitation of an inner-lining of Cu–Fe, and in some cases Zn–Fe, sulphides together with the filling in of the outer anhydrite lattice pore spaces by additional anhydrite and sulphides. Stage I precipitates anhydrite primarily composed of vent-fluid-derived Ca and seawater-derived SO_4^{-2}. Stage II precipitates the Cu–Fe sulphide minerals chalcopyrite, isocubanite, pyrite and pyrrhotite and the Zn–Fe sulphide minerals sphalerite and wurtzite from vent-fluid derived Cu, Fe, Zn and S. Weathering and biologic activity, at the seawater interface and within the pore spaces, can subsequently modify both a chimney's

composition and its morphology; but the general product of chimney growth is a layered, variably porous structure that creates nonlinear micro-environments of various temperatures and chemistries. The growth process and the layered structure of sulphide deposits make them valuable records of hydrothermal venting. However, the temporal relationships between chimney mineralogy and chemistry and vent-fluid temperature, mixing and composition are still only partially understood. Further, microbial communities within chimneys may exert their own influence on chimney growth and mineralization (Hedrick *et al.* 1992). Thus, to date, the archival utility of sulphide deposits has only been partially elucidated. Long-term *in situ* monitoring of both mineral speciation and fluid properties within hydrothermal chimneys would provide the data necessary to validate more complex models of chimney development, and could enable more detailed reconstructions of the temporal development of these potentially economically viable deep-sea mineral resources (Hoagland *et al.* 2009).

In the water column, *immediately* after seafloor venting, the mixing of high-temperature hydrothermal discharge (more than 280°C) and seawater (2–4°C) results in rapid, profuse, mineral precipitation and the production of a particle-rich mineral plume. The abiotic model of hydrothermal plume formation describes two processes (Feely *et al.* 1987; Rudnicki & Elderfield 1993; Lilley *et al.* 1995). Plume process I occurs immediately after discharge of vent fluids into the ocean: Fe(II) and other chalcophile elements co-precipitate to form polymetallic sulphide phases (i.e. a 'quenching' effect). Plume process II occurs as reduced vent fluids rise and mix with more oxidizing ambient seawater: trace elements co-precipitate with and adsorb to freshly formed Fe(III) oxyhydroxides. Plume process I results in the accumulation of seafloor metalliferous sediment deposits near vent sites and is thought to remove the major fraction of vent fluid Fe (Rudnicki & Elderfield 1993; Kadko *et al.* 1995; Field & Sherrell 2000). Process II generates a finer particle floc that can be dispersed many kilometres and is considered to be the primary mechanism for hydrothermal scavenging of seawater nutrients and trace elements (Mottl & McConachy 1990; Metz & Trefry 2000; German & Von Damm 2003). There is also a growing body of evidence that suggests that, in addition to abiotic processes, biotic—and particularly microbial—processes can be important within hydrothermal plumes (Cowen *et al.* 1986; De Angelis *et al.* 1993; Dick *et al.* 2009). For example, the most recent studies indicate that organic carbon binds a significant fraction of the dissolved and particulate metals in hydrothermal plumes by the processes of complexation (Sander *et al.* 2007; Bennett *et al.* 2009) and aggregation (Toner *et al.* 2009; Breier *et al.* submitted)—processes that have competing influences on chemical dispersal. While chemical models of hydrothermal plumes have been developed, none incorporate the full range of abiotic and biotic processes now known to occur, and none are satisfactory at predicting the behaviour of more than a subset of the elements involved in hydrothermal reactions. A more realistic model of plume chemistry may require the incorporation of both biotic and abiotic interactions and a more accurate and complete description of *in situ* plume chemical speciation.

The mixing of seawater and vent fluids that accompanies low-temperature 'diffuse flow' hydrothermal discharge (less than 20°C) leads to the production of seafloor mineral crusts and small formations of silica, barite and iron minerals. None of this low-temperature mineral precipitation is as rapid and dramatic as for high-temperature venting, but the same mixing processes also enable the growth

of extensive microbial 'mat' colonies. These microbial colonies are fuelled by fluxes of reduced Fe, Mn and S, as well as CH_4 and H_2, liberated from the lithosphere by hydrothermal circulation. The resultant 'mats' form structured microbial communities based on the redox zonation within them and the metabolic requirements of each species. Mineral forming processes are intimately related to the establishment and growth of these microbial colonies, and substrate mineralogy has been shown to influence microbial growth rates. For example, incubation experiments by Edwards *et al.* (2003) have shown that bacterial colonies grow with increasing rates on substrates of (in order, from slowest to fastest growth rate): chalcopyrite, sphalerite, pyrite, marcasite, chimney sulphide and elemental sulphur. In addition, mineralization often occurs directly on microbes themselves. A lithotrophic Fe oxidizer isolated from hydrothermal microbial mats forms ferrihydrite encrusted stalks as it grows (Emerson & Moyer 2002), and a mineral layer often covers the surface of hydrothermal microbial mats. For example, an Mn oxide crust covers the approximately 1 m thick mats at the base (5000 m deep) of Lohi Seamount. To date these mats, which are highly flocculated, have been difficult to sample and their community structure and the mineralogy of their substrate, crust and internal coatings is not well characterized, but studies are intensifying (Reysenbach *et al.* 2000; Emerson & Moyer 2002; Edwards *et al.* 2007).

3. Application of laser Raman spectroscopy in the deep sea

Raman spectroscopy is well suited to making measurements in the ocean because water is a relatively weak Raman scatterer (Williams & Collette 2001; Moore *et al.* 2009). Consequently, oceanographic applications of Raman spectroscopy are decades old. For example, the *shape* of the Raman water spectrum is temperature dependent, and has been used to measure the temperature of the upper ocean (up to a depth of 100 m) remotely, via aircraft (Leonard *et al.* 1977, 1979; Becucci *et al.* 1999). The *intensities* of Raman water spectra have also been used to determine the depth of laser penetration when correcting airborne fluorescence measurements of phytoplankton density (Bristow *et al.* 1981; Hoge & Swift 1981). It is only more recently, however, that interest has grown in using Raman spectroscopy to make chemical measurements *in situ* in both the coastal ocean and the deep sea (Kronfeldt & Schmidt 1999; Battaglia *et al.* 2004; Pasteris *et al.* 2004).

In pursuit of this, a series of sea-going Raman systems have been built (table 1). The DORISS system developed by Brewer *et al.* (2004), currently in its second generation, is based on Kaiser Optics laboratory components and uses 532 nm excitation. It was intended principally for CO_2 gas and hydrate studies. Two other sea-going Raman systems use 785 nm excitation. One of these was developed to study hydrothermal vent-fluid chemistry (Battaglia *et al.* 2004; Dable *et al.* 2006), and uses a variety of modified components including a Control Development Inc. spectrometer. The other 785 nm system was developed to detect polyaromatic hydrocarbons in seawater (Schmidt *et al.* 2004), and uses a custom surface-enhanced Raman spectroscopy probe and a Jobin Yvon spectrometer (Kronfeldt & Schmidt 1999).

Table 1. Sea-going Raman spectrometer specifications.

	spectrometer		laser		weight
	range (cm^{-1})	pixel mapping[a] (cm^{-1})	wavelength (nm)	power (mW)	in air (kg)
current systems					
Brewer *et al.* (2004)	100–4000	1	532	30	150
Battaglia *et al.* (2004)	200–2200	2	785	300	—[b]
Schmidt *et al.* (2004)	239–2739	3	785	—[b]	50
mineral specific[c]	100–1000	2	532[d]	25	<50

[a]Pixel resolution depends on optical system and is typically several times greater than pixel mapping.
[b]Not reported.
[c]Technical goal and requirements for a next-generation Raman system for hydrothermal mineral studies.
[d]Alternatively, a 785 nm wavelength laser is one of several options for minimizing fluorescence.

These choices between 532 and 785 nm excitation wavelength are worth reviewing. They reflect different choices made by the developers concerning scattering intensity, cost and fluorescence mitigation. Excitation wavelengths in the visible spectrum (350–700 nm) minimize attenuation in water; although at the short focal distances (i.e. centimetres) possible with some *in situ* applications (e.g. Breier *et al.* 2009*b*), attenuation is not significant into the near ultraviolet and infrared. Since the intensity of Raman scattering is inversely proportional to λ^4, the 532 nm wavelength lasers produces a stronger Raman scattering intensity than the less costly 785 nm wavelength lasers. However blue-green light is more likely to produce fluorescence in organic compounds, which can obscure the Raman signal. Longer excitation wavelengths, such as 785 nm, are one option for reducing fluorescence effects (Ferraro *et al.* 2003).

The DORISS system has already been used to make a variety of *in situ* measurements of gases, solids, clathrate hydrates and biomolecules. *In situ* measurements of the composition of natural gas venting in Guaymas Basin and along Hydrate Ridge have shown the composition to be primarily CH_4 (Hester *et al.* 2006). Raman spectroscopy has also been used in ocean experiments to measure rates of CO_2 dissolution (White *et al.* 2006*a*), and to determine the structure of synthetic and natural hydrates and identify the gas molecules they contain (Hester *et al.* 2006, 2007). And though the focus of this paper is on minerals, the ability for Raman spectroscopy to identify CH_4 and CO_2 is in also highly relevant to hydrothermal studies, as emissions from ultramafic-hosted hydrothermal systems are rich in volatile organic compounds and emissions from volcanic-hosted systems are rich in CO_2 (Charlou *et al.* 2002; Lupton *et al.* 2006). In addition to these gases, barite and anhydrite minerals have also been successfully identified at hydrothermal vents, as have the aragonite and calcite phases of $CaCO_3$ in seafloor shells (White *et al.* 2006*b*) and elemental sulphur in an S_8 configuration, together with beta carotenes, in seafloor bacterial mats (White *et al.* 2006*b*).

Thus, deep-sea deployments have already proven the value of *in situ* Raman systems; but deep-sea Raman applications have mainly been qualitative with the exception of White *et al.* (2006*a*), who measured CO_2 dissolution rates. While Raman spectroscopy can also be used for quantitative measurements, the approach is unlike traditional methods of analytic chemistry because absolute peak intensity is not a good basis for quantification. Raman scattering intensity is proportional to analyte concentration,

$$I_{\mathrm{R}} = I_{\mathrm{L}}\sigma\eta PC, \tag{3.1}$$

where I_{R} is the Raman scattering intensity (peak area), I_{L} is the laser intensity, σ is the Raman scattering efficiency (which is analyte specific and a function of temperature and pressure), η represents the collective instrument parameters including collection efficiency and optical throughput, P is the path length and C is the analyte concentration (Owen *et al.* 1998). However, equation (3.1) is often impractical to apply directly because instrument parameters, particularly those that affect irradiance to the sample, are difficult to keep constant (Wopenka & Pastersis 1986). In addition, for mineral crystals, Raman scattering is anisotropic, so variations in crystal orientation result in variations in peak intensity. Instead, for solids, relative chemical proportions within a sample can be quantified using 'point counting methods', where multiple measurements are made at a representative collection of points (e.g. 100 points on an evenly spaced grid), and the number of observations of each analyte are used to determine their relative proportions (Haskin *et al.* 1997; Wang *et al.* 2003). In this method, Raman bands are used to identify species; Raman intensities are not used to infer concentration.

In addition to being largely qualitative, deep-sea Raman applications to date have also focused on strong Raman scatterers such as CH_4 gas and hydrates (Hester *et al.* 2007), or dissolved analytes that can be measured by surface-enhanced Raman scattering (Schmidt *et al.* 2004). Even a short list of the most abundant hydrothermal minerals includes many that are weak Raman scatterers and share similar chemistries, and thus similar Raman spectra (figure 2; table 2). Breier *et al.* (2009*a*) conducted extensive laboratory testing to determine if these minerals could, in fact, be quantitatively distinguished in mineral mixtures. These tests used mixtures of prepared particulate standards for eight of the most common hydrothermal minerals: anhydrite, pyrite, chalcopyrite, pyrrhotite, sphalerite, hematite, magnetite and goethite. Measurements were made with a Kaiser Optics Raman instrument with a green (532 nm) excitation laser equivalent to the DORISS sea-going Raman system. An automated point counting scheme and custom autonomous spectral identification algorithm were used to quantify the composition of binary mixtures, and one seven-component mixture, of these standards. Accuracy was highest for pyrite, anhydrite and chalcopyrite (99%, 98% and 96%, respectively), good for sphalerite and magnetite (both 93%) and satisfactory for goethite and hematite (89 and 80%). For pyrrhotite, the accuracy and misidentification rate were poor; this mineral species actually includes two ideal crystal structures, and theory predicts that neither should be Raman active (Mernaugh & Trudu 1993). Thus, the results showed that quantification of laboratory standards was possible and satisfactory in most cases; but preliminary 'sea-truthing' of natural sinking and

Table 2. Deep-sea hydrothermal minerals.

sulphides		oxides, oxyhydroxides, and aluminosilicates		other minerals and compounds	
pyrite[a]	FeS_2	hematite[a]	α-Fe_2O_3	native sulphur	S_8
marcasite	FeS_2	ferrihydrite	$5Fe_2O_3 \times 9H_2O$	anhydrite[a]	$CaSO_4$
greigite	$Fe^{2+}Fe_2^{3+}S_4$	goethite[a]	α-$Fe^{3+}O(OH)$	biomolecules	
chalcopyrite[a]	$CuFeS_2$	lepidocrocite	γ-$Fe^{3+}O(OH)$		
cubanite	$CuFe_2S_3$	magnetite[a]	$Fe^{2+}Fe_2^{3+}O_4$		
isocubanite	$CuFe_2S_3$	ilmenite	$Fe^{2+}TiO_3$		
pyrrhotite[a]	$Fe_{(1\text{ to }0.83)}S$	talc	$Mg_3Si_4O_{10}(OH)_2$		
covellite	CuS	nontronite	Fe^{3+}-clay		
mackinawite	$(Fe,Ni)S_{0.9}$				
galena	PbS				
sphalerite[a]	Zn(Fe)S				
wurtzite	Zn(Fe)S				

[a]Raman spectra shown in figure 2.

suspended hydrothermal particulate samples has shown that intense broadband fluorescence frequently obscures any Raman peaks (Breier *et al.* 2009*a*). Overcoming this technical challenge would make this method more widely applicable.

4. Positioning devices and optically compatible sampling instruments

Sampling instruments are generally necessary to collect useful measurements with a sea-going Raman system. The Raman effect is weak (only 1 out of 10^8 incident photons are Raman scattered) so focused laser light is typically used to increase the intensity of incident light at the sample; even so, it can take tens of seconds to collect high-quality Raman spectra. Thus, acquiring and maintaining focus on the sample is important, and relative motion between the sample and the collection optics is detrimental to the measurements.

To enable the study of seafloor mineral and hydrate deposits, White *et al.* (2005) developed a precision underwater positioning (PUP) system for the DORISS Raman spectrometer. The PUP system is a submersible precision three-axis stage that allows the DORISS optical head to be focused on a seafloor sample of interest. The PUP system was designed to be placed directly on the seafloor by a remotely operated vehicle (ROV), to isolate measurements from submersible motion—whether from a human occupied vehicle (HOV) or an ROV. A similar positioning device could also be used to vertically profile through microbial mats, profile the interior of drill holes in massive sulphides or monitor *in situ* mineral precipitation and dissolution on rock substrates and vent organisms.

Breier *et al.* (2009*b*) developed an optically compatible, trace-metal clean, suspended-particle rosette multi-sampler for submersible-based sampling of rising hydrothermal plumes and autonomous times-series sampling of

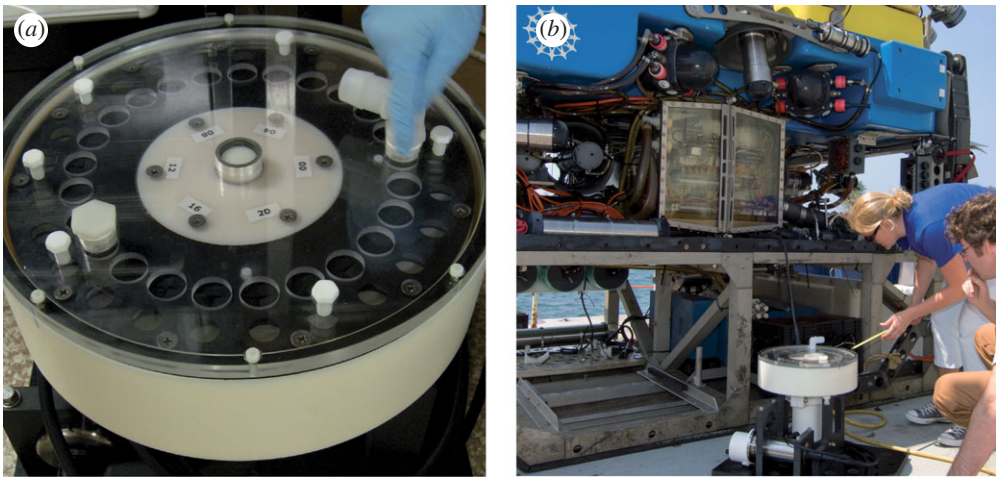

Figure 3. The SUPR sampler (*a*) is a Woods Hole Oceanographic Institution designed and built, optical-sensor compatible, multi-sample filtering head interfaced to a McLane Research Laboratories high flow-rate pumping system. An offset in the flow path provides optical access to each filtered sample; the current version has a clear acrylic housing cover and a clear polycarbonate rosette top plate, which allows collection to be monitored in real time via video link during ROV operations. When configured for ROV deployments, the SUPR system is compact enough to fit into any science payload position on ROV *Jason* (*b*). Images courtesy of Woods Hole Oceanographic Institution and Tom Kleindinst.

laterally dispersing, neutrally buoyant plumes from short moorings tethered to the seafloor (figure 3). This suspended rosette sampler (SUPR) system is designed to host *in situ* optical analysis systems, particularly for Raman spectroscopy. It solves the problems of sample geometry and control for *in situ* analysis of suspended particles by concentrating and trapping them on two-dimensional filters. These filters can be presented to the optical analysis system for as long or as often as needed and in a repeatable manner that allows for a focused beam and a minimal amount of seawater in the optical path. We are currently using this system to collect hydrothermal plume samples for shore-based analysis (Breier *et al.* submitted), but the long-term goal is to obtain *in situ* speciation measurements of suspended hydrothermal material by combining the SUPR system with an appropriate *in situ* Raman spectroscopy system.

An instrument analogous to the SUPR sampler has been developed for collecting *in situ* images of sinking particulate matter. The optical sedimentation recorder is an adaptation of the sediment trap concept, it funnels sinking particulate matter onto a flat optical plate on top of an upward looking digital camera that collects an image time series of accumulating material (Bishop *et al.* 2004; Bishop 2009). The plate surface is periodically flushed clean to prevent material buildup. This system could be readily interfaced with a sea-going Raman instrument, which would allow *in situ* speciation measurements of sinking hydrothermal material.

5. A compact laser Raman system for hydrothermal mineral analysis

As noted, the first, and second generation, sea-going Raman systems developed to date use many commercially available laboratory grade Raman components (i.e. Kaiser Optics, Jobin Yvon and Control Development Inc. spectrometers). This ensures that critical system components, such as the spectrometer, are high quality, but it also makes the systems larger and more costly than necessary for many purposes, thereby limiting their utilization. A smaller, lower-power and lower-cost sea-going Raman system optimized for mineral identification would enable many new applications of *in situ* Raman spectroscopy in deep-sea research.

In order to achieve significant size and power reduction, it is necessary to consider the minimum Raman system specifications needed to distinguish between common hydrothermal minerals. Based on the experiments of Breier *et al.* (2009*a*), the basic characteristics for a next-generation Raman system for *in situ*, long-term monitoring of hydrothermal mineralogy should have a spectral range of 100–1000 cm^{-1}, a resolution of less than 5 cm^{-1} and provide a laser power intensity of at least 5 mW on the sample. It should also incorporate some approach for minimizing fluorescence saturation and the degradation of signal to noise that it causes.

Concerning fluorescence, while green (532 nm) excitation has been successful in analysing many laboratory and *in situ* mineral samples, fluorescence has been a significant problem in some cases. Fluorescence is of a higher intensity and longer lived than Raman scattering and, thus, can overwhelm the Raman signal from a sample. Fluorescence is particularly a concern when organic matter is present—it is ubiquitous for many hydrothermal applications of interest (i.e. microbial mats). Fluorescence mitigation techniques include (i) time gating with a pulsed excitation source to differentiate between the faster, shorter Raman signal and the fluorescence signal (Matousek *et al.* 2001), (ii) basing measurements on the anti-Stokes (blue-shifted) half of the Raman spectrum that is less affected by fluorescence (which is predominantly red-shifted), and (iii) shifting to a longer wavelength excitation source (Ferraro *et al.* 2003). Of these fluorescence-mitigating approaches, time gating would significantly increase system complexity and cost, and would require higher laser powers or longer exposure times. Using the anti-Stokes half of the Raman spectrum is an intriguing option, but it is significantly less intense than the Stokes half of Raman spectrum, particularly at colder temperatures. Compensation for the weaker scattering intensity would require higher laser powers or longer exposure times. In addition, the intensity of the anti-Stokes portion of the Raman spectrum decreases rapidly with increasing Raman shift, thus there is a point where compensation is no longer practical (figure 4). This is the reason anti-Stokes Raman spectroscopy is not often used in laboratory applications. Using a red (785 nm) excitation source can mitigate fluorescence in some cases (figure 5*b*), and also lowers system cost. However the excitation produced by a red laser is less intense than that of a green laser, and red excitation does not preclude fluorescence; in fact, it too can stimulate fluorescence in some cases (figure 5*a*; White 2009). Thus, red excitation is only a partial fluorescence solution and a proper evaluation of the relative merits of red versus green excitation requires comparison of many *in situ* measurements. Therefore, what would be

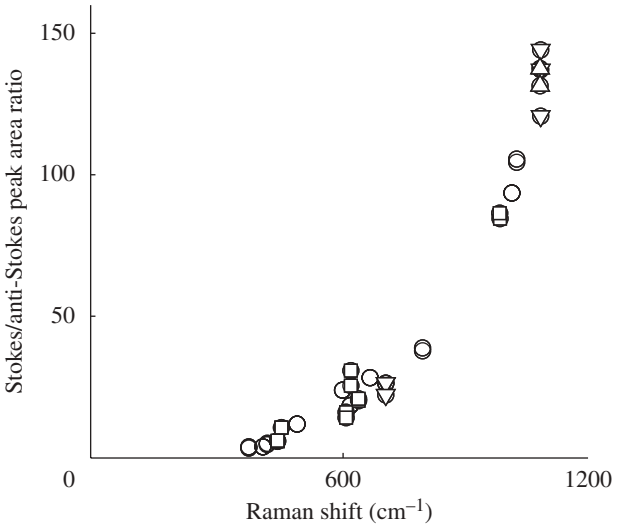

Figure 4. Raman photons are scattered to both longer (Stokes scattering) and shorter (anti-Stokes scattering) wavelengths than that of the excitation source. The anti-Stokes portion of a Raman spectrum is less influenced by fluorescence, which occurs predominantly at longer wavelengths relative to the excitation source; but the anti-Stokes portion of the Raman spectrum is significantly less intense than the Stokes portion. Area ratios for matching Stokes/anti-Stokes peaks, measured from several different minerals, show how rapidly the intensity of the anti-Stokes portion of the Raman spectrum decreases with increasing Raman shift (inverted triangle, calcite; triangle, aragonite; square, barite; open circle, anhydrite).

useful at this stage of development is a purpose-built spectrometer with an optical bench that can be reconfigured easily, to test several different excitation sources *in situ*.

6. Towards next-generation deep-sea mineralization studies

We are currently incorporating Raman spectroscopy into a laboratory analytic sequence for suspended and sinking hydrothermal plume particulate samples. That sequence begins with non-destructive elemental and speciation measurements and ends with sample digestion and bulk elemental analysis by inductively coupled plasma mass spectroscopy. These samples are collected, in part, with an instrument compatible with *in situ* optical analysis and the next step in our analytic development is to deploy a sea-going Raman system to determine the mineralogy of our samples *in situ*. Trial measurements could be made with existing technology but, as noted, further development of sea-going Raman systems, to achieve a low-cost, compact, fluorescence minimizing design, could enable a variety of new studies. The following are just three examples.

(*a*) *Long-term monitoring of sulphide chimney mineralization*

The temporal relationships between (i) hydrothermal chimney mineralogy, (ii) vent-fluid temperature, mixing and composition, and (iii) chimney-endemic microbial communities are still only partially understood. This limits the

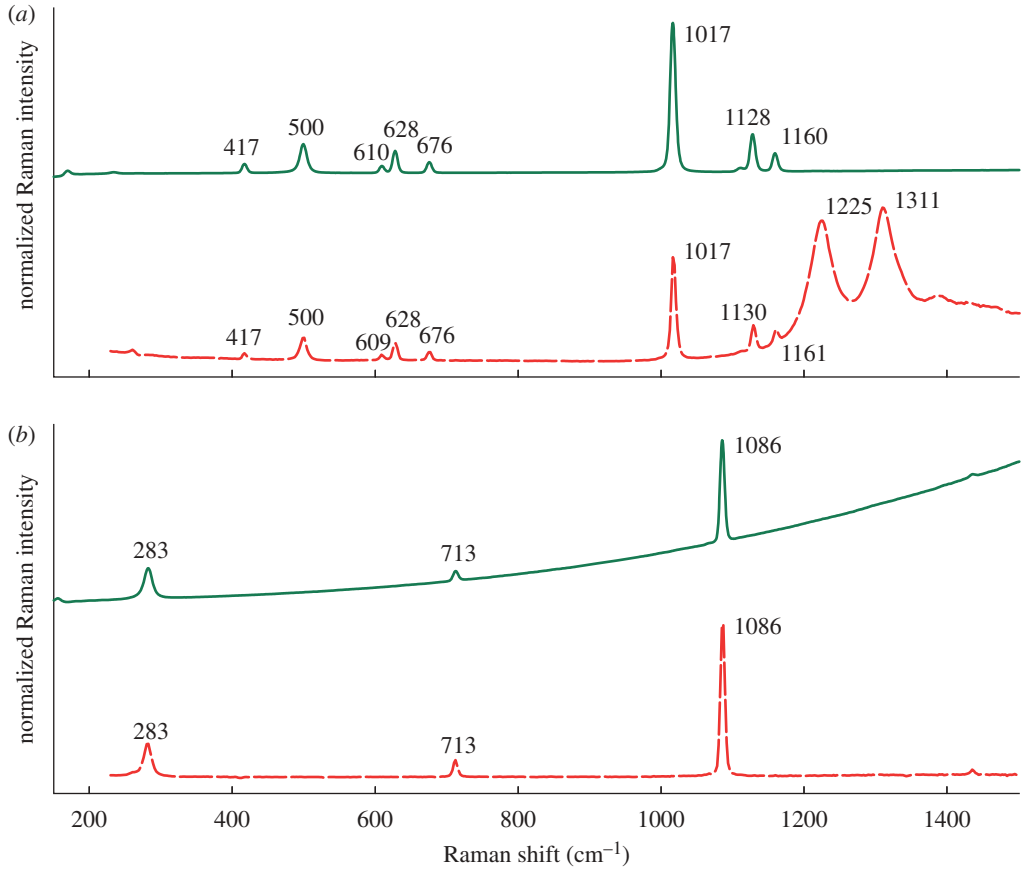

Figure 5. Red (785 nm) excitation is often used to mitigate fluorescence in Raman spectroscopy. (*a*) Raman spectra of anhydrite illustrate the fluorescence that can be induced by a red excitation source; note the narrow-band fluorescence at more than 1100 cm^{-1} and peaks at 1225 and 1311 cm^{-1} in the spectrum obtained by 785 nm excitation is absent in the spectrum obtained by 532 nm excitation. However, (*b*) Raman spectra of calcite illustrate the fluorescence reduction possible with a red excitation source; note the broad fluorescence (increasing baseline intensity) at more than 600 cm^{-1} in the spectrum obtained by 532 nm (green) excitation is absent in the spectrum obtained by 785 nm excitation. Modified from White (2009).

extent to which sulphide chimney structures can be used to reconstruct records of hydrothermal venting and makes uncertain the exact nature of the micro-environments that chimney-microbes inhabit. To better understand these relationships, recent studies have used thermocouple arrays to monitor internal temperatures within chimneys over extended periods of time (Tivey *et al.* 2002). In short, existing sulphide chimneys are broken down and removed and a thermocouple array is put in its place. A new chimney begins to form immediately, and the growth is rapid enough (several cm d^{-1}) that the thermocouple array becomes embedded within the new chimney structure within hours. Recovery of the new chimneys, along with the thermocouple arrays, allows the final chimney structure, and microbial samples therein, to be compared with the multi-point internal temperature record—but the temporal development of chimney

mineralization must still be inferred. In addition to the thermocouple array, an array of fibre-optic probes coupled to an *in situ* Raman spectrometer could allow mineral speciation to be monitored as well as temperature. In fact, such a system could be used to monitor mineralogy during a variety of seafloor mineral weathering and microbial colonization experiments. But the real value of this approach would come from multiple deployments over a variety of time scales, up to years, for which issues such as biofouling and direct mineralization on the probe heads would have to be considered along with the previously mentioned issue of fluorescence.

(*b*) *Long-term monitoring of hydrothermal plume mineral speciation*

There is an established body of research which suggests that hydrothermal flux from a given vent site along any section of mid-ocean ridge should undergo a predictable chemical evolution, linked to the underlying ridge-crest's volcano-tectonic cycles (Butterfield *et al.* 1997; Von Damm 2004). The most recent evidence supporting this kind of cyclicity comes from sediment trap samples collected following the latest eruption at the East Pacific Rise (German *et al.* 2008). However, the hypothesis remains poorly tested due to the long-term and episodic nature of volcanic eruptions and the poor temporal resolution that can be obtained from repeat 'snap-shot' sampling visits to any given area with a dedicated research submersible.

A related hypothesis, and necessary assumption if we are to infer temporal changes in hydrothermal venting from sediment traps, suspended particulate samplers, or sediment cores, is that changes in primary vent-fluid chemistry can be related, predictably, to the chemical composition of hydrothermal plume particles. This hypothesis has also not been adequately tested due to chronic under-sampling of the complete hydrothermal plume dispersal path and our inability to verify *in situ* chemical speciation. The latter point is particularly worrisome because kinetically limited reactions and meta-stable minerals are probable results of the rapid, turbulent mixing and steep chemical and thermal gradients produced by hydrothermal venting. As noted, the sampling technology exists to collect hydrothermal plume samples, both sinking and suspended, over the course of months and years—and even to do so in a manner that allows optical access to the samples during collection. With the commencement of science operations on the Neptune Canada cabled seafloor observatory, such sampling packages, deployed at the main endeavour vent field, may finally be able to be directed and monitored in response to volcano-tectonic activity on the Juan de Fuca plate. Raman spectrometers, coupled to these particle sampling packages, could allow the actual *in situ* mineral speciation of collected samples to be identified immediately, and any variability in this mineralogy could also be monitored, in real time, for periods of up to 6–12 months between necessary maintenance and servicing.

(*c*) *Point measurements and vertical profiling for mineral identification within microbial mats*

Deep-sea microbial mat research is still nascent and both (i) the relationships between microbial mat community structure, substrate and surface crust mineralogy and (ii) the processes of internal mat mineralization remain poorly

understood. However the study of deep-sea microbial mats, motivated in part by the search for novel metabolic processes, is becoming more intensive, and new sampling instruments are being developed to better sample and measure the chemistry of these systems. A sampling system currently being developed by J. Breier and D. Emerson (Bigelow Laboratory for Ocean Sciences) will allow high-resolution vertical profiling within microbial mats for both sample collection and measurement of dissolved O_2 and temperature. An ability to determine *in situ* mineral speciation would provide a very valuable additional measurement with which to characterize the environment and, hence, serve as a guide for more detailed sampling. This, however, may represent the ultimate challenge for *in situ* deep-sea Raman spectroscopy because the possibility for significant fluorescence from the predominantly organic microbial matrix is very high.

7. Conclusions

For a variety of geological studies, understanding mineral speciation can be at least as important as determining elemental concentrations of a given material. Mineral speciation is particularly important in deep-sea hydrothermal environments where steep chemical and thermal gradients, rapid and turbulent mixing and biologic processes produce a multitude of diverse mineral phases—many only metastable. Laser Raman spectroscopy is, in many ways, well suited to mineral speciation measurements in the deep sea. A particular strength of Raman spectroscopy for deep-sea hydrothermal systems is that it allows for *in situ*, non-invasive and non-destructive measurements of Fe and Mn compounds. This could enable measurements of thermodynamically unstable phases to be made, *in situ*, and provide a novel method for the long-term monitoring of variations in hydrothermal Fe and Mn compounds. As such, Raman spectroscopy has great potential as a tool in a variety of hydrothermal science applications. Indeed, sea-going Raman systems have been built and used to make a variety of measurements in the deep sea, but there is a real need for further development. To realize the full potential of this technique for hydrothermal research, a small, low-cost sea-going Raman system optimized for mineral identification, which also incorporates a fluorescence-minimizing design, is required. Such a tool could be used to track chemical transformations of Fe/Mn-rich minerals within developing sulphide deposits, hydrothermal plumes and growing microbial mats, and could be deployed in a variety of fashions: in autonomous experimental packages, as part of a cabled or moored observatory, or from a deep-diving research submersible: HOV, ROV or even an Autonomous Underwater Vehicle (AUV). The experimental approaches this would enable could greatly improve our understanding of: (i) the impact of Fe and Mn cycling upon global ocean chemistry, (ii) the extent to which Fe- and Mn-oxidation energy can fuel (micro)biogeochemical cycling within the water column above hydrothermal vent sites, and (iii) the mechanisms by which depositional records of the history of hydrothermal discharge are laid down and preserved in massive sulphide deposits and deep ocean sediments.

We acknowledge discussions with, and help from, Peter Brewer, Meg Tivey, Olivier Rouxel, Lauren Mullineaux, Anna-Louise Reysenbach, the LADDER 2007, MAR 2008 and ELSC 2009 scientific parties (NSF OCE-0424953, NSF OCE-0728391, OCE-0752469, OCE-0751839), as well

as financial support from the US National Science Foundation (NSF OCE-0550331). The Woods Hole Oceanographic Institution's Deep Ocean Exploration Institute funded initial construction of the SUPR-sampler.

References

Alt, C. J. 1995 Subseafloor processes in mid-ocean ridge hydrothermal systems. In *Seafloor hydrothermal systems: physical, chemical, biological and geological interactions*. Washington, DC: American Geophysical Union.

Battaglia, T. M., Dunn, E. E., Lilley, M. D., Holloway, J., Dable, B. K., Marquardt, B. J. & Booksh, K. S. 2004 Development of an *in situ* fiber optic Raman system to monitor hydrothermal vents. *Analyst* **129**, 602–606. (doi:10.1039/b404505j)

Becucci, M., Cavalieri, S., Eramo, R., Fini, L. & Materazzi, M. 1999 Accuracy of remote sensing of water temperature by Raman spectroscopy. *Appl. Opt.* **38**, 928–931. (doi:10.1364/AO.38.000928)

Bennett, S. A., Rouxel, O., Schmidt, K., Garbe-Schonberg, D., Statham, P. J. & German, C. R. 2009 Iron isotope fractionation in a buoyant hydrothermal plume, 5° S Mid-Atlantic Ridge. *Geochim. Cosmochim. Acta* **73**, 5619–5634. (doi:10.1016/j.gca.2009.06.027)

Bishop, J. K. B. 2009 Autonomous observations of the ocean biological carbon pump. *Oceanography* **22**, 182–193.

Bishop, J. K. B., Wood, T. J., Davis, R. E. & Sherman, J. T. 2004 Robotic observations of enhanced carbon biomass and export at 55° S during SOFeX. *Science* **304**, 417–420. (doi:10.1126/science.1087717)

Breier, J. A., German, C. R. & White, S. N. 2009*a* Mineral phase analysis of deep-sea hydrothermal particulates by a Raman Spectroscopy Expert Algorithm (RaSEA): towards autonomous *in situ* exploration and experimentation. *Geochem. Geophys. Geosyst.* **10**, Q05T05. (doi:10.1029/2008GC002314)

Breier, J. A., Rauch, C. G., McCartney, K., Toner, B. M., Fakra, S. C., White, S. N. & German, C. R. 2009*b* A suspended-particle rosette multi-sampler for discrete biogeochemical sampling in low-particle-density waters. *Deep-Sea Res. I* **56**, 1579–1589. (doi:10.1016/j.dsr.2009.04.005)

Breier, J. A., Toner, B. M., Fakra, S., Manganini, S. J. & German, C. R. Submitted. The influence of micro-aggregate formation on deep-sea hydrothermal plume chemistry and particle transport: 9° 50′ N East Pacific Rise. *Earth Planet. Sci. Lett.*

Brewer, P. G., Malby, G., Pasteris, J. D., White, S. N., Peltzer, E. T., Wopenka, B., Freeman, J. & Brown, M. O. 2004 Development of a laser Raman spectrometer for deep-ocean science. *Deep Sea Res. I* **51**, 739–753. (doi:10.1016/j.dsr.2003.11.005)

Bristow, M., Nielson, D., Bundy, D. & Furtek, R. 1981 Use of water Raman emission to correct airborne laser fluorosensor data for effects of water optical attenuation. *Appl. Opt.* **20**, 2889–2906. (doi:10.1364/AO.20.002889)

Butterfield, D. A. *et al.* 1997 Seafloor eruptions and evolution of hydrothermal fluid chemistry. *Phil. Trans. R. Soc. Lond. A* **355**, 369–386. (doi:10.1098/rsta.1997.0013)

Charlou, J. L., Donval, J. P., Fouquet, Y., Jean-Baptiste, P. & Holm, N. 2002 Geochemistry of high H_2 and CH_4 vent fluids issuing from ultramafic rocks at the Rainbow hydrothermal field (36°14′ N, MAR). *Chem. Geol.* **191**, 345–359. (doi:10.1016/S0009-2541(02)00134-1)

Corliss, J. B. *et al.* 1979 Submarine thermal springs on the Galápagos rift. *Science* **203**, 1073–1083. (doi:10.1126/science.203.4385.1073)

Cowen, J. P., Massoth, G. J. & Baker, E. T. 1986 Bacterial scavenging of Mn and Fe in a mid-field to far-field hydrothermal particle plume. *Nature* **322**, 169–171. (doi:10.1038/322169a0)

Dable, B. K., Love, B. A., Battaglia, T. M., Booksh, K. S., Lilley, M. D. & Marquardt, B. J. 2006 Characterization and quantitation of a tertiary mixture of salts by Raman spectroscopy in simulated hydrothermal vent fluid. *Appl. Spectrosc.* **60**, 773–780. (doi:10.1366/000370206777887125)

De Angelis, M. A., Lilley, M. D. & Baross, J. A. 1993 Methane oxidation in deep-sea hydrothermal plumes of the Endeavour segment of the Juan de Fuca Ridge. *Deep Sea Res. I* **40**, 1169–1186. (doi:10.1016/0967-0637(93)90132-M)

Dick, G. J., Andersson, A. F., Baker, B. J., Simmons, S. L., Thomas, B. C., Yelton, A. P. & Banfield, J. F. 2009 Community-wide analysis of microbial genome signatures. *Gen. Biol.* **10**, R85. (doi:10.1186/gb-2009-10-8-r85)

Edwards, K. J., McCollom, T. M., Konishi, H. & Busek, P. R. 2003 Seafloor bioalteration of sulfide minerals: results from *in situ* incubation studies. *Geochim. Cosmochim. Acta* **67**, 2843–2856. (doi:10.1016/S0016-7037(03)00089-9)

Edwards, K. J., Moyer, C. L., Chan, C., Emerson, D. & Horn, G. 2007 The Loihi Seamount microbial observatory: an extremely common deep-sea habitat for Fe-oxidizing bacteria. *Geochim. Cosmochim. Acta* **71**, A249–A301. (doi:10.1016/j.gca.2007.06.015)

Elderfield, H. & Schultz, A. 1996 Mid-ocean ridge hydrothermal fluxes and the chemical composition of the ocean. *Annu. Rev. Earth Planet. Sci.* **24**, 191–224. (doi:10.1146/annurev.earth.24.1.191)

Emerson, D. & Moyer, C. L. 2002 Neutrophilic Fe-oxidizing bacteria are abundant at the Loihi Seamount hydrothermal vents and play a major role in Fe oxide deposition. *Appl. Environ. Microbiol.* **68**, 3085–3093. (doi:10.1128/AEM.68.6.3085-3093.2002)

Feely, R. A., Lewison, M., Massoth, G. J., Robertbaldo, G., Lavelle, J. W., Byrne, R. H., Vondamm, K. L. & Curl, H. C. 1987 Composition and dissolution of black smoker particulates from active vents on the Juan de Fuca ridge. *J. Geophys. Res. Solid Earth Planets* **92**, 11 347–11 363.

Ferraro, J. R., Nakamoto, K. & Brown, C. W. 2003 *Introductory Raman spectroscopy*. New York, NY: Academic Press.

Field, M. P. & Sherrell, R. M. 2000 Dissolved and particulate Fe in a hydrothermal plume at 9°45′ N, East Pacific Rise: slow Fe(II). *Geochim. Cosmochim. Acta* **64**, 619–628. (doi:10.1016/S0016-7037(99)00333-6)

Fisher, C. R. 1995 Toward an appreciation of hydrothermal-vent animals: their environment, physiological ecology, and tissue stable isotope values. In *Seafloor hydrothermal systems: physical, chemical, biological and geological interactions*. Washington, DC: American Geophysical Union.

Fortin, D. & Langley, S. 2005 Formation and occurrence of biogenic iron-rich minerals. *Earth-Sci. Rev.* **72**, 1–19. (doi:10.1016/j.earscirev.2005.03.002)

German, C. R. & Von Damm, K. L. 2003 Hydrothermal processes. In *Treatise on geochemistry*. Amsterdam, The Netherlands: Elsevier.

German, C. R., Rouxel, O. J. & Edwards, K. J. 2008 Time-series study of post-eruption vent-fluxes: EPR 9° 50′ N. *Eos Trans. AGU* **89**, Fall Meet. Suppl., Abstract V53D-01.

Goldfarb, M. S., Converse, D. R., Holland, H. D. & Edmond, J. M. 1983 The genesis of hot spring deposits on the East Pacific Rise, 21° N. *Econ. Geol. Monograph* **5**, 184–197.

Hannington M. D., Jonasson, I. R., Herzig, P. M. & Petersen, S. 1995 Physical and chemical processes of seafloor mineralization at mid-ocean ridges. In *Seafloor hydrothermal systems: physical, chemical, biological and geological interactions*. Washington, DC: American Geophysical Union.

Haskin, L. A., Wang, A., Rockow, K. M., Jolliff, B. L., Korotev, R. L. & Viskupic, K. M. 1997 Raman spectroscopy for mineral identification and quantification for *in situ* planetary surface analysis: a point count method. *J. Geophys. Res.* **102**, 19 293–19 306. (doi:10.1029/97JE01694)

Haymon, R. M. & Kastner, M. 1981 Hot-spring deposits on the East Pacific Rise at 21° N: preliminary description of mineralogy and genesis. *Earth Planet. Sci. Lett.* **53**, 363–381. (doi:10.1016/0012-821X(81)90041-8)

Haymon, R. M. *et al.* 1993 Volcanic eruption of the mid-ocean ridge along the East Pacific Rise crest at 9°45–52′N: direct submersible observations of sea-floor phenomena associated with an eruption event in April, 1991. *Earth Planet. Sci. Lett.* **119**, 85–101. (doi:10.1016/0012-821X(93)90008-W)

Hedrick, D. B., Pledger, R. D., White, D. C. & Baross, J. A. 1992 *In situ* microbial ecology of hydrothermal vent sediments. *FEMS Microbiol. Ecol.* **101**, 1–10. (doi:10.1111/j.1574-6968.1992.tb05755.x)

Hessler, R. R. & Kaharl, V. A. 1995 The deep-sea hydrothermal vent community: an overview. In *Seafloor hydrothermal systems: physical, chemical, biological and geological interactions.* Washington, DC: American Geophysical Union.

Hester, K. C., White, S. N., Peltzer, E. T., Brewer, P. G. & Sloan, E. D. 2006 Raman spectroscopic measurements of synthetic gas hydrates in the ocean. *Mar. Chem.* **98**, 304–314. (doi:10.1016/j.marchem.2005.09.006)

Hester, K. C., Dunk, R. M., White, S. N., Brewer, P. G., Peltzer, E. T. & Sloan, E. D. 2007 Gas hydrate measurements at Hydrate Ridge using Raman spectroscopy. *Geochim. Cosmochim. Acta* **71**, 2947–2959. (doi:10.1016/j.gca.2007.03.032)

Hoagland, P., Beaulieu, S., Tivey, M. A., Eggert, R. G., German, C. R., Glowka, L. & Lin, L. 2009 Deep-sea mining of seafloor massive sulfides. *Mar. Policy.*

Hoge, F. E. & Swift, R. N. 1981 Airborne simultaneous spectroscopic detection of laser-induced water Raman backscatter and fluorescence from chlorophyll a and other naturally occurring pigments. *Appl. Opt.* **20**, 3197–3205. (doi:10.1364/AO.20.003197)

Janecky, D. R. & Seyfried, W. E. 1984 Formation of massive sulfide deposits on oceanic ridge crests—incremental reaction models for mixing between hydrothermal solutions and seawater. *Geochim. Cosmochim. Acta* **48**, 2723–2738. (doi:10.1016/0016-7037(84)90319-3)

Kadko, D. 1993 An assessment of the effect of chemical scavenging within submarine hydrothermal plumes upon ocean geochemistry. *Earth Planet. Sci. Lett.* **120**, 361–374. (doi:10.1016/0012-821X(93)90250-D)

Kadko, D, Baross, J. & Alt, J. 1995 The magnitude and global implications of hydrothermal flux. In *Seafloor hydrothermal systems: physical, chemical, biological and geological interactions.* Washington, DC: American Geophysical Union.

Kronfeldt, H. D. & Schmidt, H. 1999 Submersible fiber-optic sensor system for coastal monitoring. *Sea Technol.* **40**, 51–55.

Leonard, D. A., Caputo, B. & Johnson, R. L. 1977 Experimental remote sensing of subsurface temperature in natural ocean water. *Geophys. Res. Lett.* **4**, 279–281. (doi:10.1029/GL004i007p00279)

Leonard, D. A., Caputo, B. & Hoge, F. E. 1979 Remote sensing of subsurface water temperature by Raman scattering. *Appl. Opt.* **18**, 1732–1745. (doi:10.1364/AO.18.001732)

Lilley, M. D., Feely, R. A. & Trefry, J. H. 1995 Chemical and biochemical transformations in hydrothermal plumes. In *Seafloor hydrothermal systems: physical, chemical, biological and geological interactions*. Washington, DC: American Geophysical Union.

Lupton, J. *et al.* 2006 Submarine venting of liquid carbon dioxide on a Mariana Arc volcano. *Geochem. Geophys. Geosyst.* **7**, Q08007. (doi:10.1029/2005GC001152)

Maginn, E. J., Little, C. T. S., Herrington, R. J. & Mills, R. A. 2002 Sulphide mineralisation in the deep sea hydrothermal vent polychaete, *Alvinella pompejana*: implications for fossil preservation. *Mar. Geol.* **181**, 337–356. (doi:10.1016/S0025-3227(01)00196-7)

Matousek, P., Towrie, M., Ma, C., Kwok, W. M., Phillips, D., Toner, W. T. & Parker, A. W. 2001 Fluorescence suppression in resonance Raman spectroscopy using a high-performance picosecond Kerr gate. *J. Raman Spectrosc.* **3**, 983–988. (doi:10.1002/jrs.784)

Mernaugh, T. P. & Trudu, A. G. 1993 A laser Raman microprobe study of some geologically important sulphide minerals. *Chem. Geo.* **103**, 113–127. (doi:10.1016/0009-2541(93)90295-T)

Metz, S. & Trefry, J. H. 2000 Chemical and mineralogical influences on concentrations of trace metals in hydrothermal fluids. *Geochim. Cosmochim. Acta* **64**, 2267–2279. (doi:10.1016/S0016-7037(00)00354-9)

Moore, C., Barnard, A., Fietzek, P., Lewis, M. R., Sosik, H. M., White, S. & Zielinski, O. 2009 Optical tools for ocean monitoring and research. *Ocean Sci.* **5**, 661–684.

Mottl, M. J. & McConachy, T. F. 1990 Chemical processes in buoyant hydrothermal plumes on the East Pacific Rise near 21° N. *Geochim. Cosmochim. Acta* **54**, 1911–1927. (doi:10.1016/0016-7037(90)90261-I)

Owen, H., Battery, D. E., Pelletier, M. J. & Slater, S. 1998 New spectroscopic instrument based on volume holographic optical elements. *Proc. SPIE* **2406**, 260–267.

Pasteris, J. D., Wopenka, B., Freeman, J. J., Brewer, P. G., White, S. N., Peltzer, E. T. & Malby, G. E. 2004 Raman spectroscopy in the deep ocean: successes and challenges. *Appl. Spectrosc.* **58**, 195–208. (doi:10.1366/0003702041389319)

Reysenbach, A. L., Banta, A. B., Boone, D. R., Cary, S. C. & Luther, G. W. 2000 Microbial essentials at hydrothermal vents. *Nature* **404**, 835. (doi:10.1038/35009029)

Rudnicki, M. D. & Elderfield, H. 1993 A chemical model of the buoyant and neutrally buoyant plume above the TAG vent field, 26 degrees N, Mid-Atlantic Ridge. *Geochim. Cosmochim. Acta* **57**, 2939–2957. (doi:10.1016/0016-7037(93)90285-5)

Sander, S. G., Koschinsky, A., Massoth, G., Stott, M. & Hunter, K. A. 2007 Organic complexation of copper in deep-sea hydrothermal vent systems. *Environ. Chem.* **4**, 81–89. (doi:10.1071/EN06086)

Schmidt, H., Ha, N. B., Pfannkuche, J., Amann, H., Kronfeldt, H. D. & Kowalewska, G. 2004 Detection of PAHs in seawater using surface-enhanced Raman scattering (SERS). *Mar. Pollut. Bull.* **49**, 229–234. (doi:10.1016/j.marpolbul.2004.02.011)

Scott, S. D. & Barnes, H. L. 1972 Sphalerite-wurtzite equilibria and stoichiometry. *Geochim. Cosmochim. Acta* **36**, 1275–1295. (doi:10.1016/0016-7037(72)90049-X)

Tivey, M. K. 1995 Modelling chimney growth and associated fluid flow at seafloor hydrothermal vent sites. In *Seafloor hydrothermal systems: physical, chemical, biological and geological interactions*. Washington, DC: American Geophysical Union.

Tivey, M. K., Bradley, A. M., Joyce, T. M. & Kadko, D. 2002 Insights into tide-related variability at seafloor hydrothermal vents from time-series temperature measurements. *Earth Planet. Sci. Lett.* **202**, 693–707. (doi:10.1016/S0012-821X(02)00801-4)

Toner, B. M., Fakra, S. C., Manganini, S. J., Santelli, C. M., Marcus, M. A., Moffett, J., Rouxel, O., German, C. R. & Edwards, K. J. 2009 Preservation of iron(II) by carbon-rich matrices in a hydrothermal plume. *Nat. Geosci.* **2**, 197–201. (doi:10.1038/ngeo433)

Von Damm, K. L. 2004 Evolution of the hydrothermal systems at East Pacific Rise 9° 50′ N: geochemical evidence for changes in the upper oceanic crust. In *Mid-ocean ridges: hydrothermal interactions between the lithosphere and oceans*. Washington, DC: American Geophysical Union.

Wang, A. *et al.* 2003 Development of the Mars microbeam Raman spectrometer (MMRS), *J. Geophys. Res.* **108**, 505. (doi:10.1029/2002JE001902)

White, S. N. 2009 Laser Raman spectroscopy as a technique for identification of seafloor hydrothermal and cold seep minerals. *Chem. Geol.* **259**, 240–252. (doi:10.1016/j.chemgeo.2008.11.008)

White, S. N., Kirkwood, W. J., Sherman, A. D., Brown, M. O., Henthorn, R., Salamy, K. A., Walz, P. M., Peltzer, E. T. & Brewer, P. G. 2005 Development and deployment of a precision underwater positioning system for *in situ* laser Raman spectroscopy in the deep ocean. *Deep-Sea Res. I* **52**, 2376–2389. (doi:10.1016/j.dsr.2005.09.002)

White, S. N., Brewer, P. G. & Peltzer, E. T. 2006*a* Determination of gas bubble fractionation rates in the deep ocean by laser Raman spectroscopy. *Mar. Chem.* **99**, 12–23. (doi:10.1016/j.marchem.2004.10.006)

White, S. N., Dunk, R. M., Brewer, P. G., Peltzer, E. T. & Freeman, J. J. 2006*b* *In situ* Raman analyses of deep-sea hydrothermal and cold seep systems (Gorda Ridge & Hydrate Ridge). *Geochem. Geophys. Geosyst.* **7**, Q05023. (doi:10.1029/2005GC001204)

Williams, T. L. & Collette, T. W. 2001 Environmental applications of Raman spectroscopy to aqueous systems. In *Handbook of Raman spectroscopy* (*Practical spectroscopy*). New York, NY: Marcel Dekker, Inc.

Wolery, T. J. & Sleep, N. H. 1976 Hydrothermal circulation and geochemical flux at mid-ocean ridges. *J. Geol.* **84**, 249–275. (doi:10.1086/628195)

Wopenka, B. & Pastersis, J. D. 1986 Limitations to quantitative analysis of fluid inclusions in geological samples by laser Raman microprobe spectroscopy. *Appl. Spectrosc.* **40**, 144–151. (doi:10.1366/0003702864509592)